PERGAMON

Energy Conversion & Management 40 (1999) 1441–1461

ENERGY CONVERSION & MANAGEMENT

Solar desalination based on humidification process—II. Computer simulation

Naser Kh. Nawayseh[a,*], Mohammed Mehdi Farid[b], Abdul Aziz Omar[c], Ahmad Sabirin[c]

[a] *School of Industrial Technology, University Sains Malaysia, 11800, Penang, Malaysia*
[b] *Department of Chemical & Material Engineering, The University of Auckland, Auckland, New Zealand*
[c] *School of Chemical Engineering, University Sains Malaysia, 31750, Tronoh, Perak, Malaysia*

Received 23 April 1998; accepted 21 December 1998

Abstract

Solar desalination requires an efficient method of evaporation and condensation at relatively low temperatures. This could be suitably achieved in a humidification/dehumidification process using circulated air to enhance evaporation of the water. With proper utilization of the latent heat of condensation of water vapor, the process efficiency could be made high. In order to optimize the design of such a desalination unit, a simulation program was constructed in which the set of non-linear equations describing the desalination unit were solved numerically. The results of the simulation were in agreement with the experimental results of two different units constructed in Jordan and Malaysia. The performance of each unit was tested when they were operated with an energy obtained either from solar or an electrical heating source. The air flow rate was found to have an insignificant effect on the productivity of desalinated water. The simulation allows the proper choice of the feed water flow rate to the unit. © 1999 Elsevier Science Ltd. All rights reserved.

Keywords: Solar; Desalination; Humidification; Simulation

* Corresponding author. Present address: Department of Automatic Control and Systems Engineering, The University of Sheffield, Mappin Street, Sheffield S1 3JD, UK. Fax: +44-114-273-1729.
E-mail address: COP98NKN@sheffield.ac.uk (N.Kh. Nawayseh)

PII: S0196-8904(99)00017-5

Nomenclature

A_{cond}	surface area of condenser (m^2)
A_{unit}	surface area of desalination unit (m^2)
A_{col}	gross area of solar collector (m^2)
a	humidifier surface area per unit volume (m^2/m^3)
Cp_w	specific heat capacity of water (J/kg K)
C_{unit}	specific heat capacity of unit (J/kg K)
G	air mass flow rate (kg/s)
H	enthalpy of air (J/kg)
I_T	solar radiation intensity received by collector (W/m^2)
i	time counter in stepwise computation
K	mass transfer coefficient in humidifier (kg/m^2 s)
L	water mass flow rate (kg/s)
M_{unit}	mass of unit (kg)
Q_{heater}	heating power supplied by heater (watt)
T	temperature (°C)
T_{amb}	ambient temperature (°C)
U_{cond}	overall heat transfer coefficient (W/m^2 K)
U_{loss}	heat loss coefficient (W/m^2 K)
V	volume of humidifier (m^3)
Δt	time increment (second)
η_{col}	collector efficiency (dimensionless)

Subscripts

1	condenser water inlet
2	condenser water outlet
3	humidifier water inlet
4	humidifier water outlet
5	air at bottom of unit
6	air at top of unit

1. Introduction

Nawayseh et al. [1] have shown that the humidification–dehumidification process, described in part I of this work, is an efficient method of solar desalination. The units, based on such a process, usually consist of two vertical ducts connected from the top and the bottom ends to form a closed loop for air circulation. The units may be operated in a forced or natural draft mode. A large surface condenser is usually fixed in one of the ducts, while wooden packing is used in the other duct for efficient humidification of the air. The saline water is fed to the condenser to condense partially the water vapor from the air. The latent heat of condensation is used to preheat the feed water, which is further heated in a flat plate solar collector before it is sprayed over the wooden packing in the humidifier. The air is continuously heated and humidified, then partially dehumidified in the condenser. The desalinated water is collected from the bottom of the condenser, while the warm brine is rejected from the bottom of the humidifier. A sketch of such a desalination process is shown in Fig. 1.

Pilot and bench desalination units were constructed and tested in Jordan by Al-Hallaj [2]. The details of the units are given in the mentioned reference. The two units were operated under steady state conditions using an electrical heater to heat the water. The pilot unit was also operated under the unsteady state mode using solar energy as a heat source. In the steady state operation, air in the unit was circulated either by natural draft or forced draft using an electrical fan, while only natural draft was employed in the solar heating mode. Another unit was constructed and operated in Malaysia, based on the same principle, but with a different construction, as described in part I of this work. These units of single stage were designed to provide warm water for domestic use in addition to the desalinated water obtained. The productivity has been shown to increase significantly by using a multi-stage humidification process [3]. Even with a single stage, a high production of 10 to 12 l/m^2day was reported by Refs. [4,5]. However, Refs. [2,6,7] have reported lower production rates on similar single stage desalination units. The variation in the productivity of the existing units suggests the requirement to study their performance in detail.

The main objective of this work was to construct a simulation program that could be used in the design of this type of desalination unit. This will allow the study of the effect of the different parameters on the performance of these units. The results of the simulation program

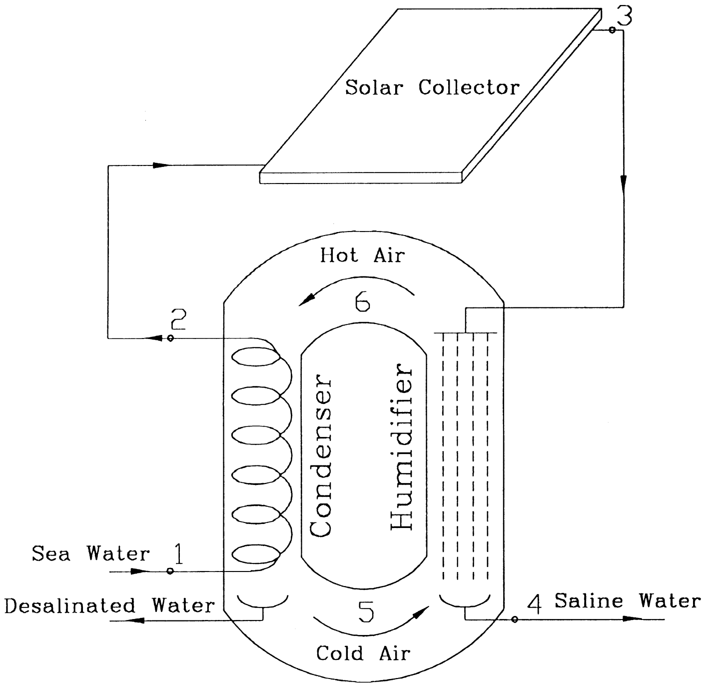

Fig. 1. Sketch of the desalination process.

will be tested against the experimental measurements obtained from the three mentioned desalination units. In part I of this work, empirical and theoretical correlations were developed to describe the heat and mass transfer in the condensers and humidifiers. These correlations were used in the simulation, as described in the following section.

2. The simulation program

In this paper, two types of simulation have been discussed, the steady state and the unsteady state. The first was used to test the performance of the desalination unit when electrical heating was the source of heat. The second was used when a flat plate solar collector was the heat source. The unit constructed in Malaysia by Nawayseh [8] was operated with natural draft air circulation only, while the unit constructed in Jordan by Al-Hallaj [2] was operated with both natural and forced draft. All these modes of operation were tested by the simulation program developed in this work.

The following five equations were used to describe the heat balance and the rate of heat transfer in the condenser, humidifier and electrical heater:

$$LCp_w(T_2 - T_1) + 0.5U_{loss}A_{unit}\left(\frac{T_5 + T_6}{2} - T_{amb}\right) = G(H_6 - H_5) \tag{1}$$

$$LCp_w(T_2 - T_1) = U_{cond}A_{cond}\left[\frac{(T_6 - T_2) - (T_5 - T_1)}{\ln\dfrac{T_6 - T_2}{T_5 - T_1}}\right] \tag{2}$$

$$LCp_w(T_3 - T_4) - 0.5U_{loss}A_{unit}\left(\frac{T_5 + T_6}{2} - T_{amb}\right) = G(H_6 - H_5) \tag{3}$$

$$G(H_6 - H_5) = KaV\left[\frac{(H_3 - H_6) - (H_4 - H_5)}{\ln\dfrac{H_3 - H_6}{H_4 - H_5}}\right] \tag{4}$$

$$Q_{heater} = LCp_w(T_3 - T_2) \tag{5}$$

In the unsteady state simulation, the heat balance on the heater defined by Eq. (5) was replaced by the heat balance on the solar collector:

$$I_TA_{col}\eta_{col} = \frac{M_{unit}C_{unit}}{\Delta t}\left[\left(\frac{T_5 + T_6}{2}\right)_{i+1} - \left(\frac{T_5 + T_6}{2}\right)_i\right] + U_{loss}A_{unit}\left[\frac{T_5 + T_6}{2} - T_{amb}\right] + LCp_w(T_4 - T_1) \tag{6}$$

The l.h.s in Eq. (6) represents the useful energy obtained from the collector. The first term on the r.h.s represents the energy stored (or lost) in the wall of the unit during a specified time

Table 1
The fixed parameters used in the simulation for the three units constructed in Malaysia and Jordan

Reference	Condenser surface area (m^2)	Humidifier surface area (m^2)	Humidifier surface area per unit volume (m^2/m^3)	Height of the unit (m)	Solar collector area (m^2)	U_{loss} (W/m^2 K)
Nawayseh [8] (Pilot unit)	8.9	11.9	58	3	2.77	1.0
Al-Hallaj [2] (Pilot unit)	4 (single) 8 (double)	5.04	14	2	2.0	1.0
Al-Hallaj [2] (Bench unit)	0.6 (single) 1.2 (double)	0.96	87	1	—	1.2

interval. This includes the heat stored in the condenser plate and the tubes filled with water. The second term describes the total heat losses from the unit wall to the ambient, which is twice the heat loss term shown in Eq. (1) or (3). In writing the above equations, the following assumptions were made:

1. The air enters the humidifier saturated and leaves saturated. This has been verified from the experimental measurements.
2. The log-mean temperature difference of the temperature and enthalpy may be used to simplify the computation. This will avoid the requirement of point to point calculations in both the condenser and humidifier for each time increment during the whole simulation time.
3. In the calculations of the heat loss from the units, the wall was assumed at the same temperature as the humid air flowing along it, which is a reasonable assumption due to the heavy insulation used. For this purpose, it was also assumed that the air temperature varied linearly from the bottom to the top of the unit. The same assumption was used in the calculation of the heat stored in the wall.
4. In the natural air circulation mode, the air velocity was too small to be measured by any available method. In the steady state simulation, the air velocity was calculated from Eq. (1) using the experimentally measured parameters. In the unsteady state simulation, an average value for the air velocity during the whole day was used. Further work would be required to develop an independent equation for predicting the air velocity in terms of the buoyancy and the frictional losses through the humidifier and condenser. However, a small error in the measured air velocity would have only limited effect on the results of the simulation, as will be discussed later in this paper.

The empirical and theoretical correlations developed in part I of this work were used to calculate the mass and heat transfer coefficients required in Eqs. (2) and (4). The loss coefficient U_{loss} was measured and calculated theoretically for the different units [2,8]. The measured values were used in the simulations. Table 1 shows the values of all the fixed parameters used in the simulation program for the three units. The enthalpy and humidity of the saturated air were calculated using the following empirical correlation developed from reported data [9].

$$H = 0.00585T^3 - 0.497T^2 + 19.87T - 207.61 \tag{7}$$

$$W = 2.19 * 10^{-6}T^3 - 1.85 * 10^{-4}T^2 + 7.06 * 10^{-3}T - 0.077 \tag{8}$$

3. Results of the steady state simulation

Eqs. (1)–(5) were solved using Newton's method of solution of a non-linear system of equations. The LINPAC subroutine [10] was used for this purpose. In the computer program, the heating rate, water and air flow rates, ambient temperature and the initial guess of all the temperatures were introduced as input to the computer program. The error criterion (usually taken as 0.00001) and the number of equations to be solved were also introduced to the program. The operating variables T_2 to T_6 were calculated, until the specified accuracy was achieved. The desalination rate was calculated from the estimated humidity of the air at the top and bottom of the unit.

The excellent agreement between the experimental values of the temperatures and those obtained from the simulation is shown in Fig. 2 for one of the units. Similar agreements were found for the other units. The excellent agreement may be due to the fact that the correlation of the mass transfer coefficient used was developed from the same measurements. However, the heat transfer coefficient in the condenser was calculated theoretically and was not based on the measured values. Fig. 3 shows a comparison between the measured and the calculated desalination production of the three units, as obtained from the simulation program. Considering the fact that the units were of different sizes and designs, the prediction is good for both the natural and forced draft air circulation, with little under prediction.

The temperatures in the simulation program, as well as the production rate, were found to

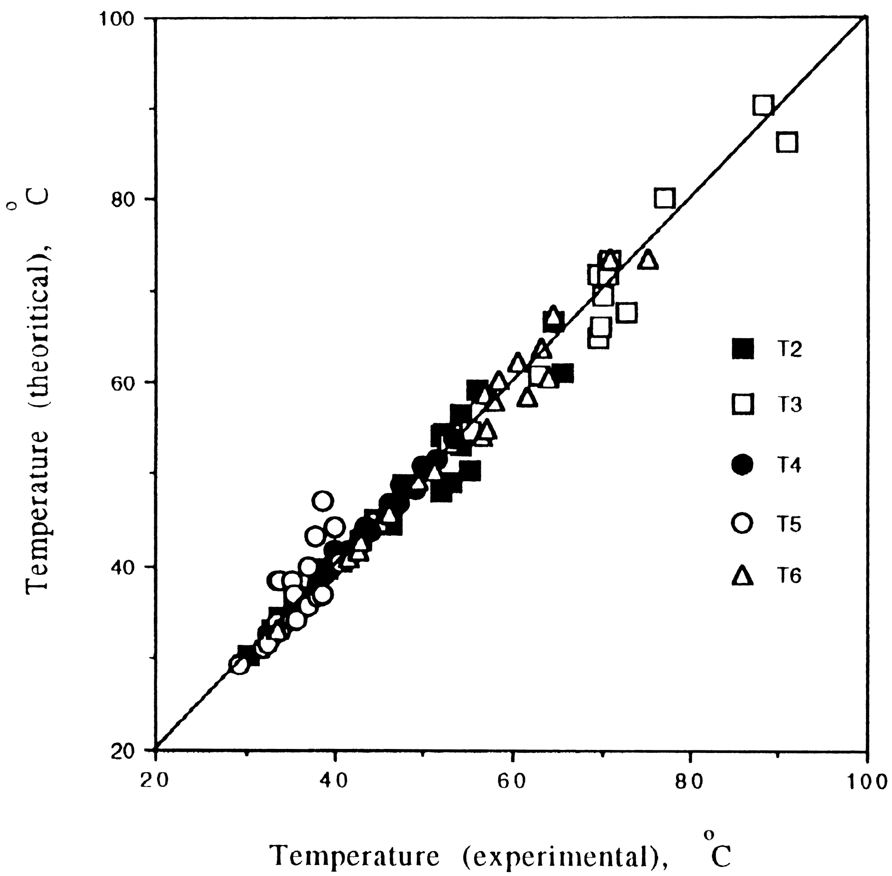

Fig. 2. Prediction of the steady state water and air temperatures in the desalination unit constructed in Malaysia.

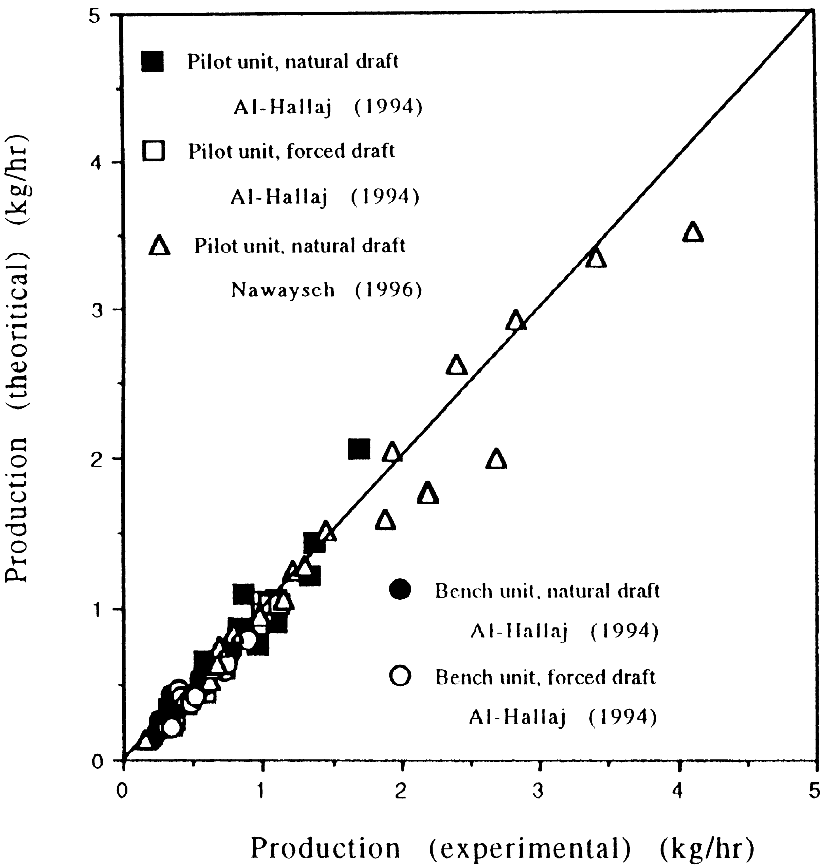

Fig. 3. Prediction of the desalination rate in the three desalination units.

converge fast to the correct values even if the initial guesses of the temperatures were far from the true values. Fig. 4 shows the computational paths for the operating temperature T_3 with two initial guesses of high and low temperatures. The figure shows that the initial two guesses converge fast to the same final value. Similar trends were found with the other temperatures. The convergence of Newton's method is represented by the internal iteration shown in Fig. 4 by the data having the same symbol. The external iterations (usually three) were necessary for correction of the calculated overall heat transfer coefficient. Fig. 5 shows the corresponding estimates of the production rate, showing a convergence to a single value independent of the initial guess.

Figs. 6 and 7 show the effect of air mass flow rate on the production rate and estimated temperatures. Increasing the air flow rate up to three times that of the natural draft air circulation has decreased mainly the air temperature at the top of the unit, and to a lesser extent, the production rate. The results belong to both steady and unsteady state simulations. When the air mass flow rate was reduced below the natural draft estimate, then the calculated values of H_6 could exceed those of H_3, causing the program to halt. The results also show that

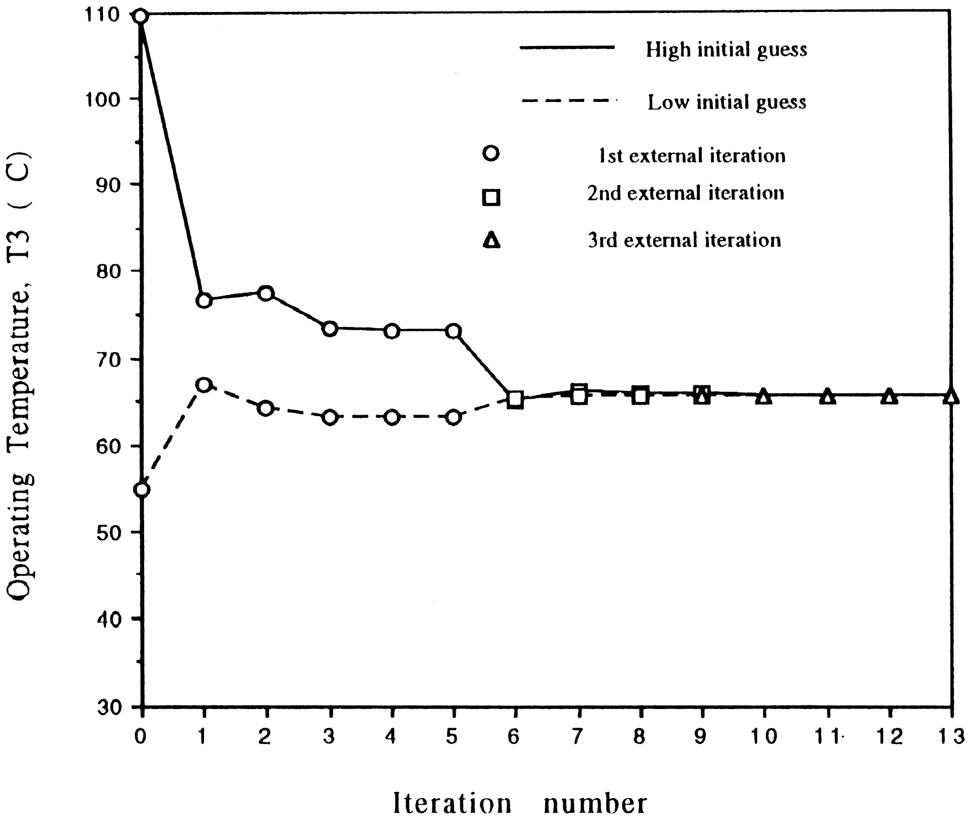

Fig. 4. Computational convergence of the operating temperature T_3 using high and low initial guesses.

the air flow rate has no effect on the temperature of the water leaving the humidifier T_4, since this temperature is totally governed by the overall energy balance represented by Eq. (6).

4. Results of the unsteady state simulation

The unsteady state simulation program describes the true performance of any solar desalination unit of the type described in this paper. In the simulation program, Eq. (5) was replaced by Eq. (6) describing the collector performance. The collector efficiency was calculated from the following equations developed for the different collectors used:

$$\eta_{col} = 0.44 - 0.0028\left(\frac{T_2 - T_{amb}}{I_T}\right) \tag{9}$$

$$\eta_{col} = 0.60 - 0.0078\left(\frac{T_2 - T_{amb}}{I_T}\right) \tag{10}$$

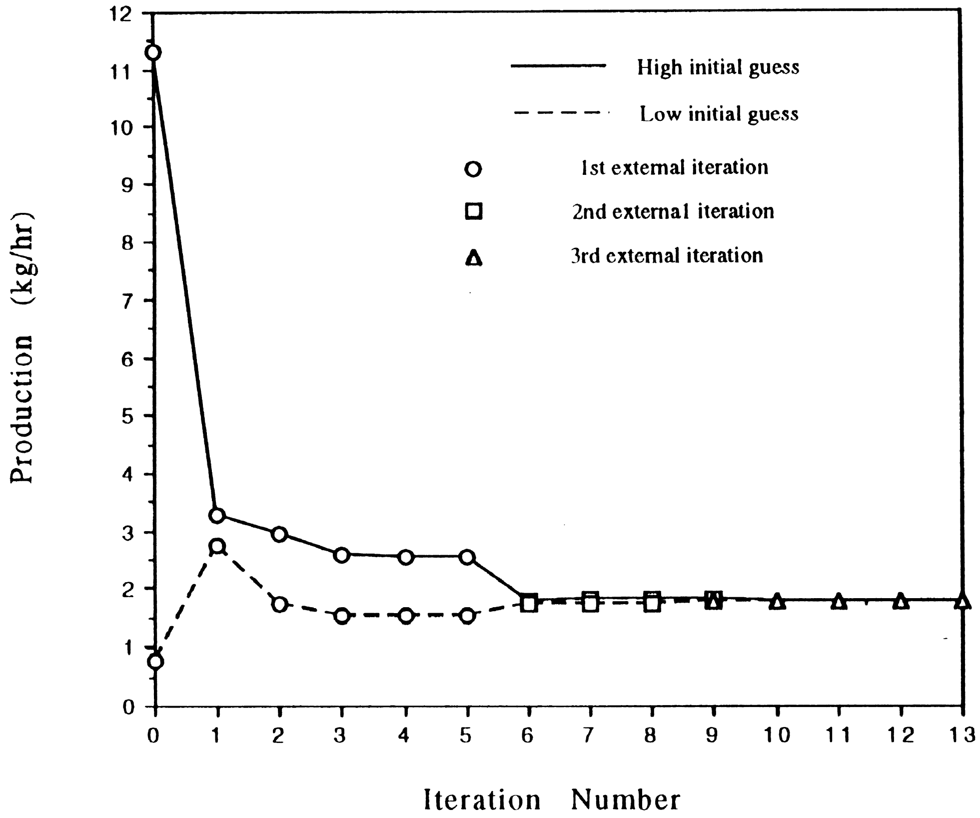

Fig. 5. Computational convergence of the production based on high and low temperature guesses.

The flow maldistribution of water in the collector, due to the low water flow rate used, might have been another reason for the low efficiency. In Malaysia, the intermittent cloudy weather caused big fluctuations in the solar radiation received, which could have been another reason for the low collector efficiency. The flat plate solar collector efficiencies, as reported by Hsieh [11], are usually higher than that given by the above equations. However, the reported efficiencies were for the collector without its associated piping.

The results of three simulations are shown in Figs. 8 to 15, for the pilot units constructed in Jordan and Malaysia. Fig. 8 shows the solar radiation on inclined surfaces for typical days in Malaysia, Jordan and Iraq as measured by Nawayseh [8], Al-Hallaj [2] and Farid and Hammad [12], respectively. The average ambient temperatures were 32°, 25° and 43°C, respectively. The measurements with high collection efficiency reported by Ref. [12] were used to test the performance of the unit constructed in Malaysia when subjected to high solar radiation. In that measurement, electrical heating was used to simulate the true useful energy obtained from the collector, as reported by the mentioned reference. The observed two hours shift in the measured solar radiation in Malaysia was partly due to the one hour shift usually done in Iraq and Jordan, and partly due to the cloud appearing in the morning of that day.

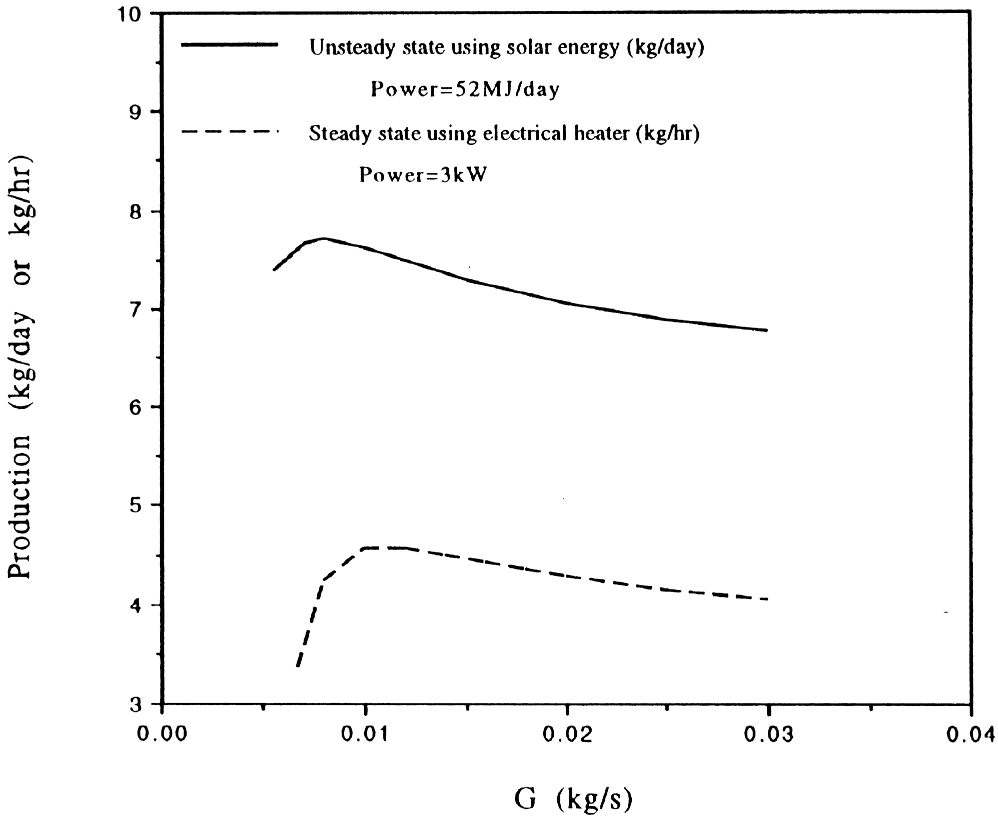

Fig. 6. Simulation study for the effect of air flow rate on the hourly and daily production of the desalination unit.

Figs. 9–11 show a comparison between the measured and the estimated air and water temperatures in the desalination units. Ambient and water inlet temperatures were also included in the figures. The theoretical prediction is reasonable, considering the assumptions and simplifications made. The same may be said with respect to the estimated production of the units as shown in Figs. 12 and 13. The measured solar radiation and the ambient temperature were expressed by Fourier series for use in the simulation program. However, their values were assumed constant during the 10 min selected for the stepwise calculations. It was not possible to use the true solar radiation, due to the large fluctuation in the values. The rapid change in the solar intensity shown in Fig. 8 caused instability in the computation, as may be seen from the set of equations presented earlier.

The simulation program was also used to test some of the steady state measurements as shown in Fig. 14. The time reported for the pilot unit constructed in Jordan to reach steady state was about 6 h, while the corresponding time for the unit constructed in Malaysia was less than 4 h. This is due to the lower heat capacity of the walls of the unit constructed in Malaysia. The results agreed well with the prediction of the simulation program as shown in Fig. 14.

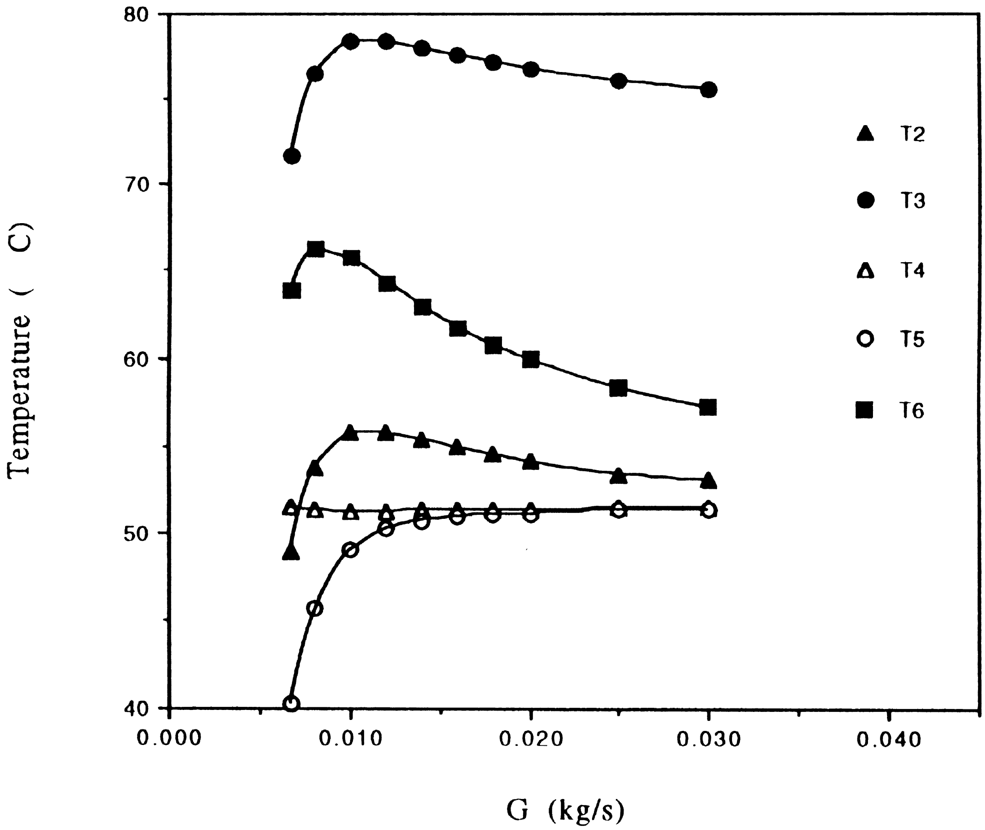

Fig. 7. Simulation study for the effect of air flow rate on the air and water temperatures of the desalination unit.

The effect of water flow rate was also studied and found significant on the production. The increase of water flow rate increases the heat and mass transfer coefficients significantly. It also lowers the operating temperatures in the unit and in the solar collector. This has two opposite effects, as it leads to a higher collector efficiency but lower evaporation and condensation efficiency. The maximum production shown in Fig. 15, as obtained from the simulation study, is the result of these factors. Such maximum has been observed experimentally [2].

5. Conclusion

It was possible to predict the performance of some desalination units constructed at two different places with different geometry and size. The five equations describing the humidifier, the condenser and the solar collector were solved numerically. The effect of air flow rate on the desalination production was found small, which is in agreement with the experimental observations. Increasing the water flow rate was found to decrease production due to the lower

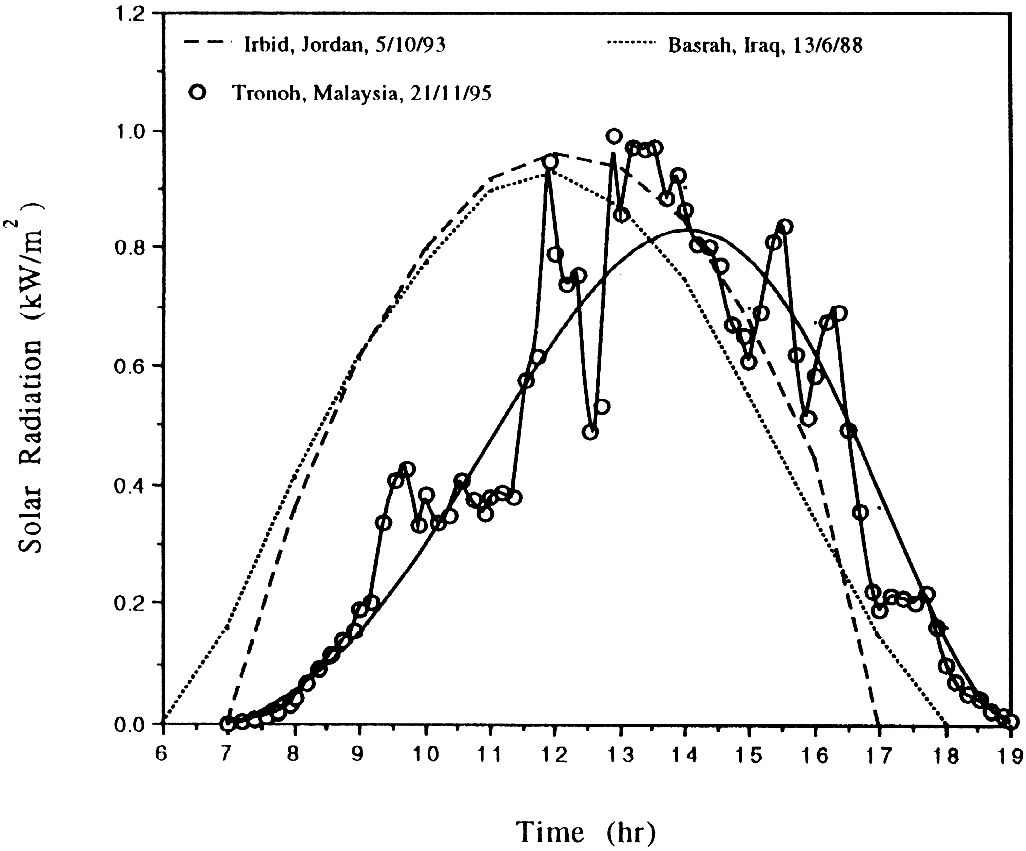

Fig. 8. Solar radiation measurements at different locations.

evaporation caused by the lower temperature. However, reducing the water flow rate to extreme values was found to lower the production due to the dramatic drop in the collector efficiency at high temperatures. The simulation program showed fast convergence of the temperatures and production rate to the final values irrespective of the initial guesses.

Acknowledgements

The authors would like to acknowledge the financial support of this work by the University Sains Malaysia.

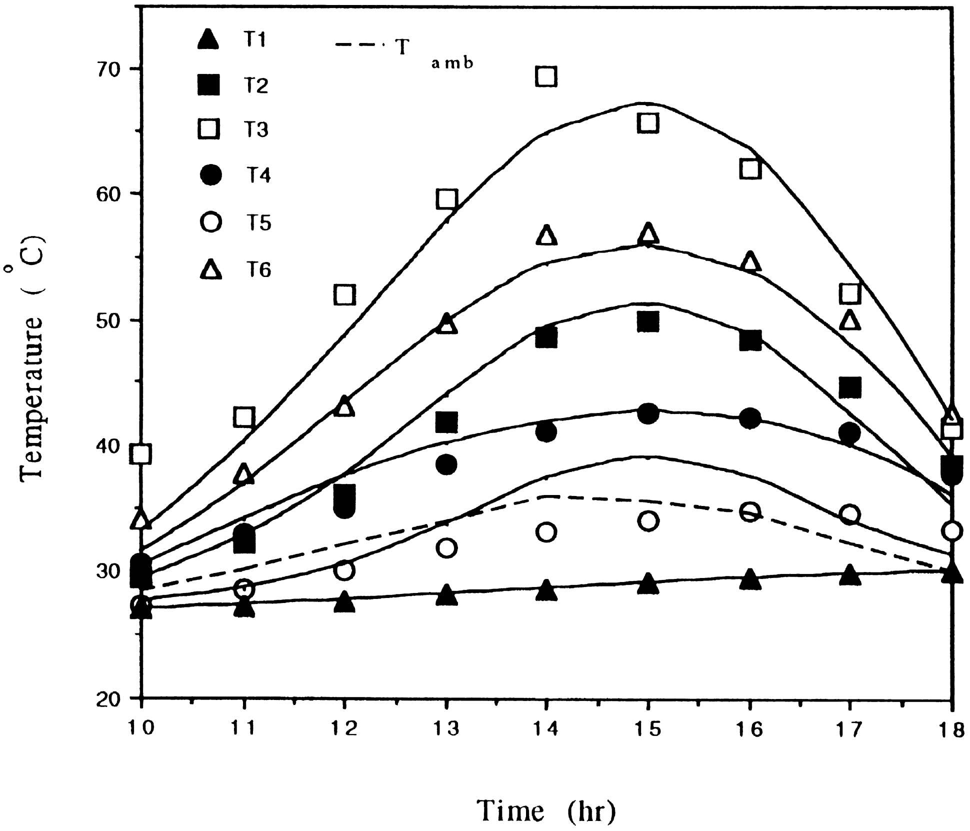

Fig. 9. Prediction of the water and air temperatures in the desalination unit constructed in Malaysia.

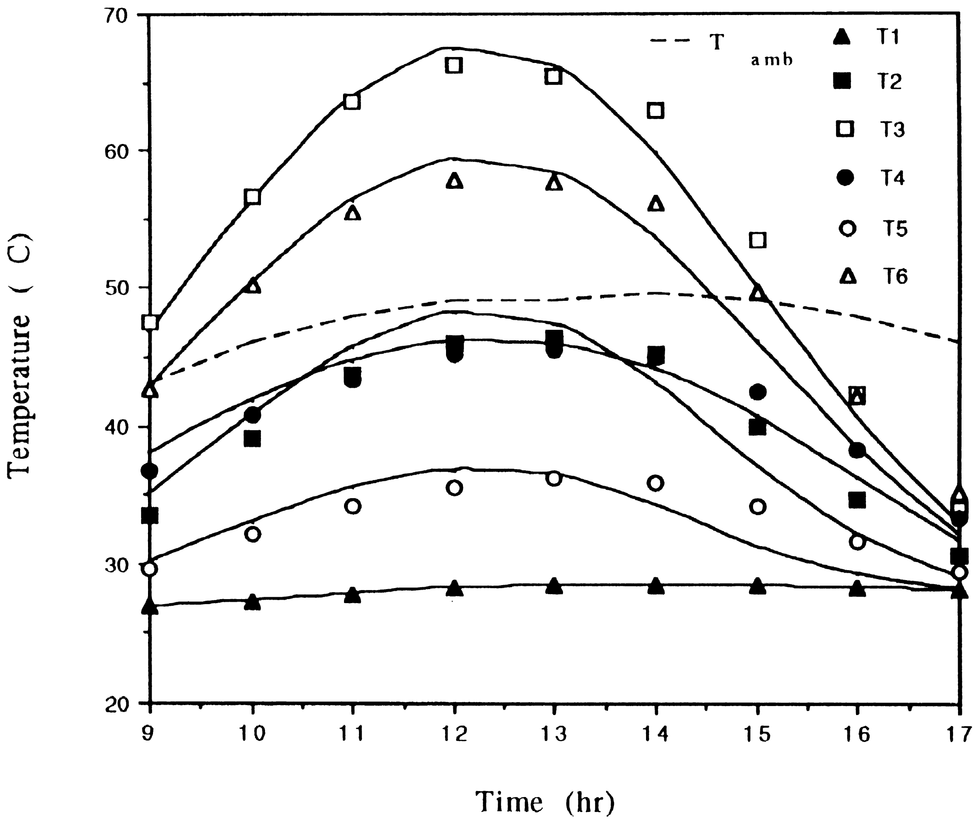

Fig. 10. Prediction of the water and air temperatures in the desalination unit constructed in Malaysia when operated with high solar radiation.

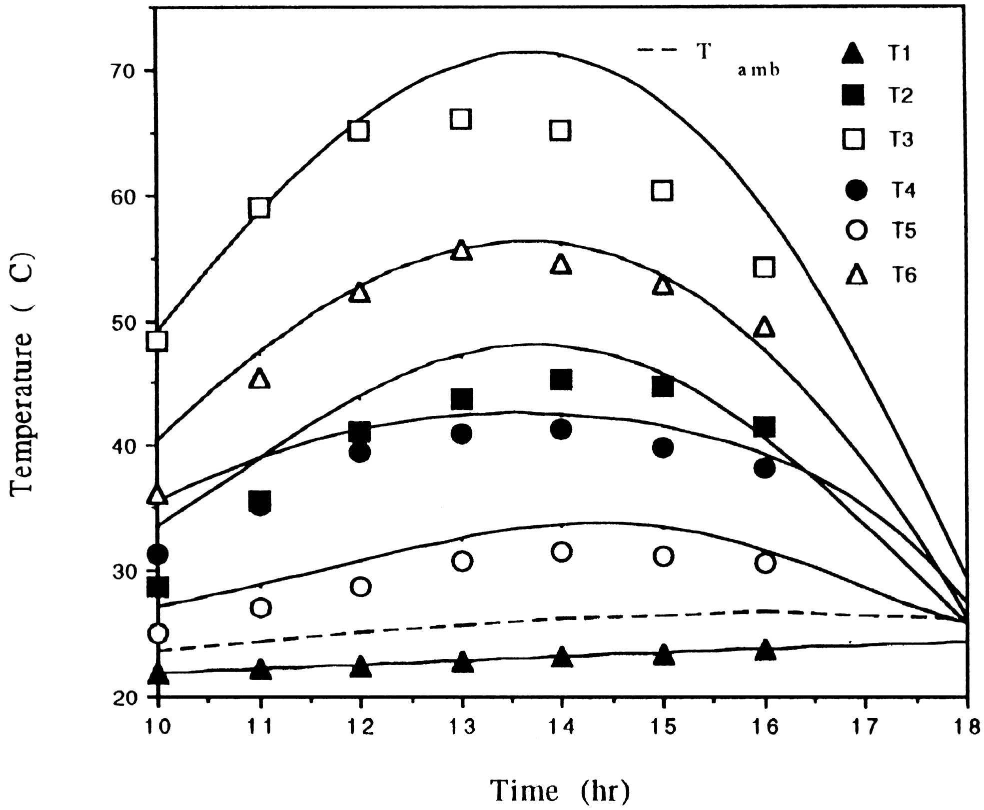

Fig. 11. Prediction of the water and air temperatures in the unit constructed in Jordan.

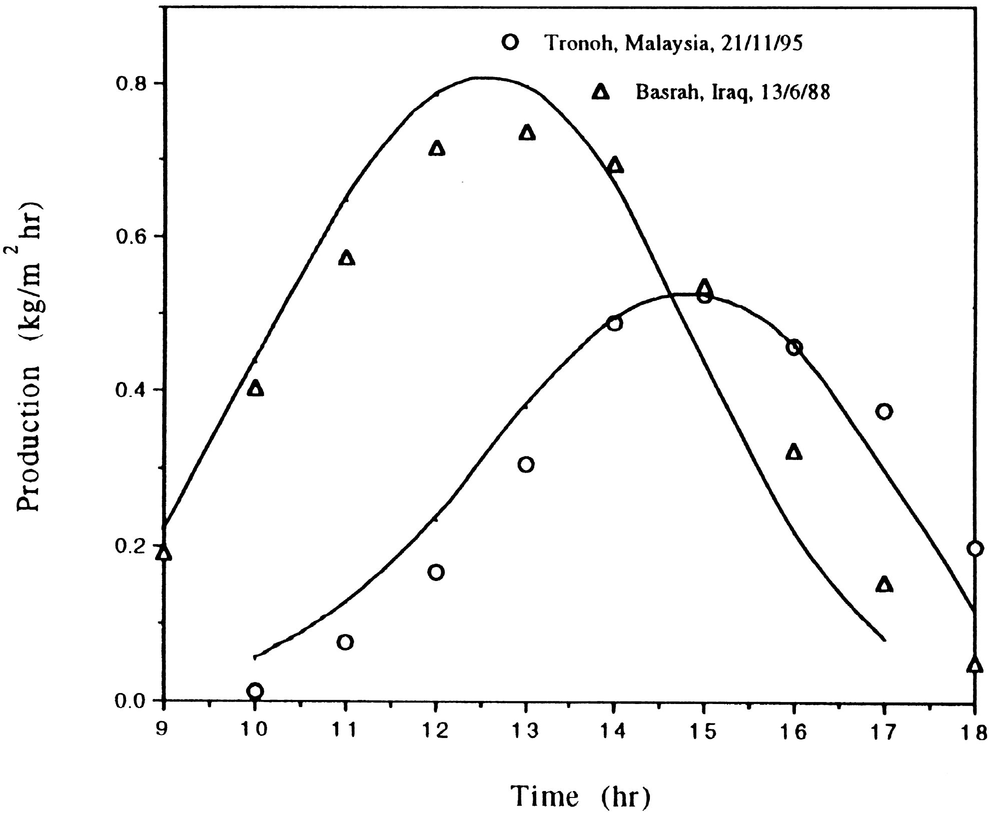

Fig. 12. Prediction of the desalination rate in the unit constructed in Malaysia and operated under two different solar radiations.

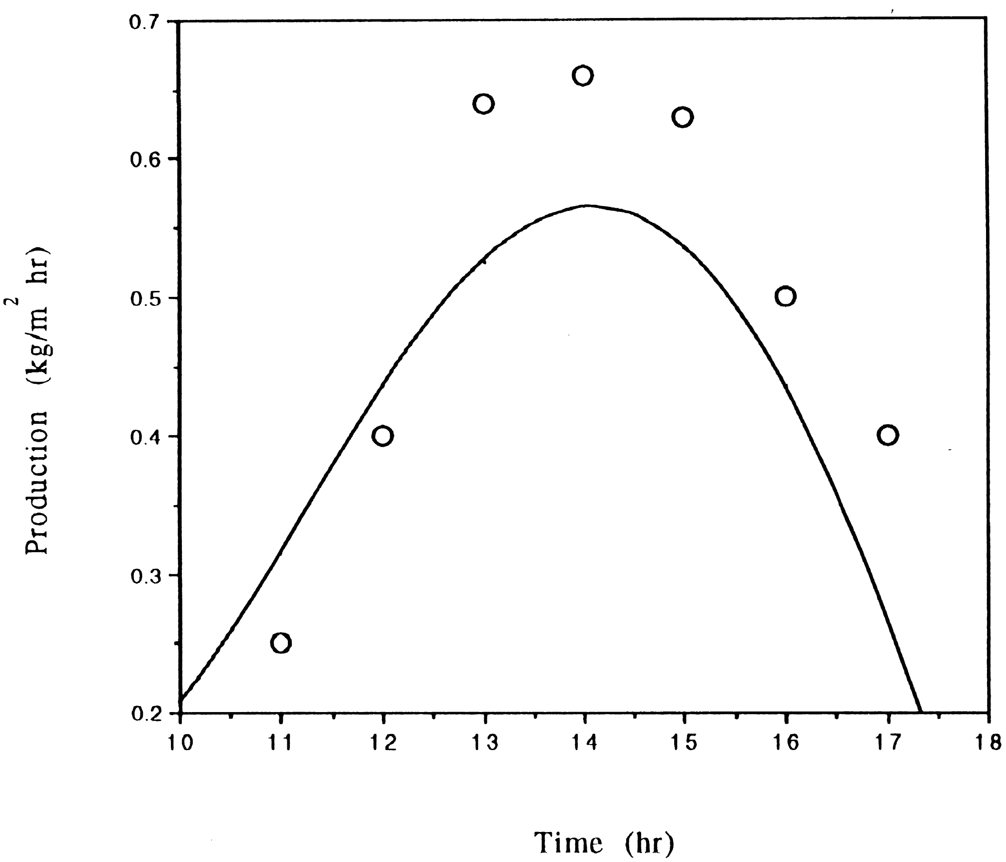

Fig. 13. Prediction of the desalination rate in the unit constructed in Jordan.

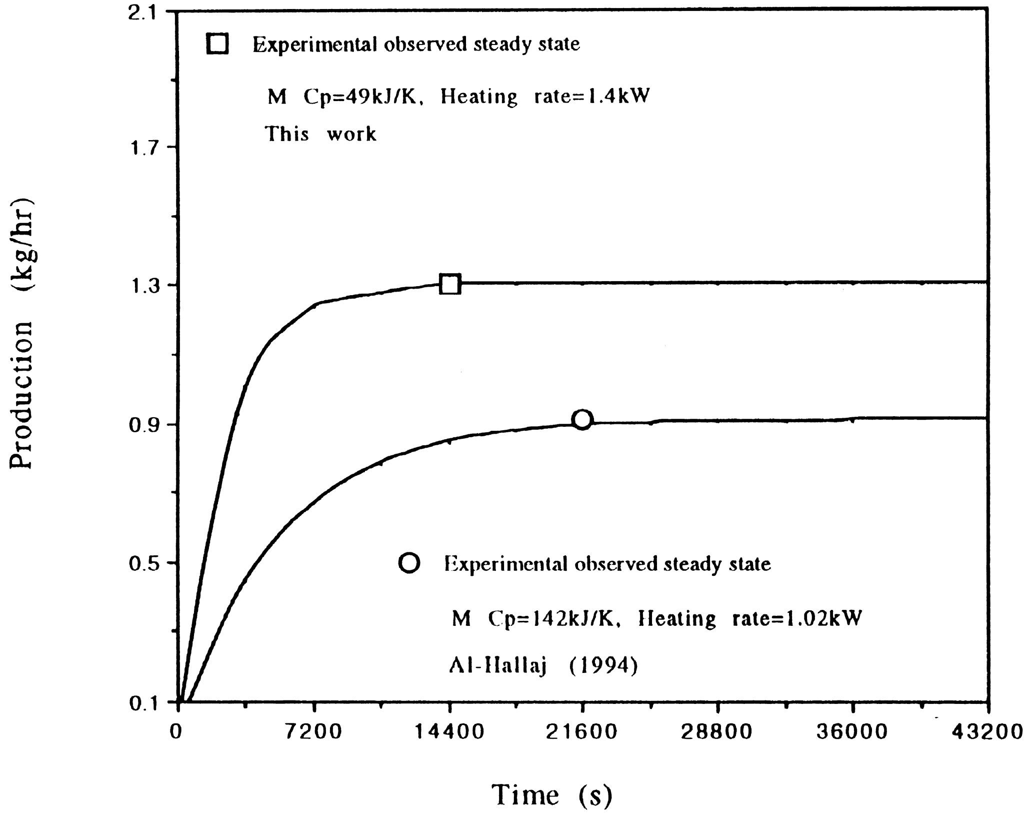

Fig. 14. The approach to steady state for two pilot units having walls of different heat capacity.

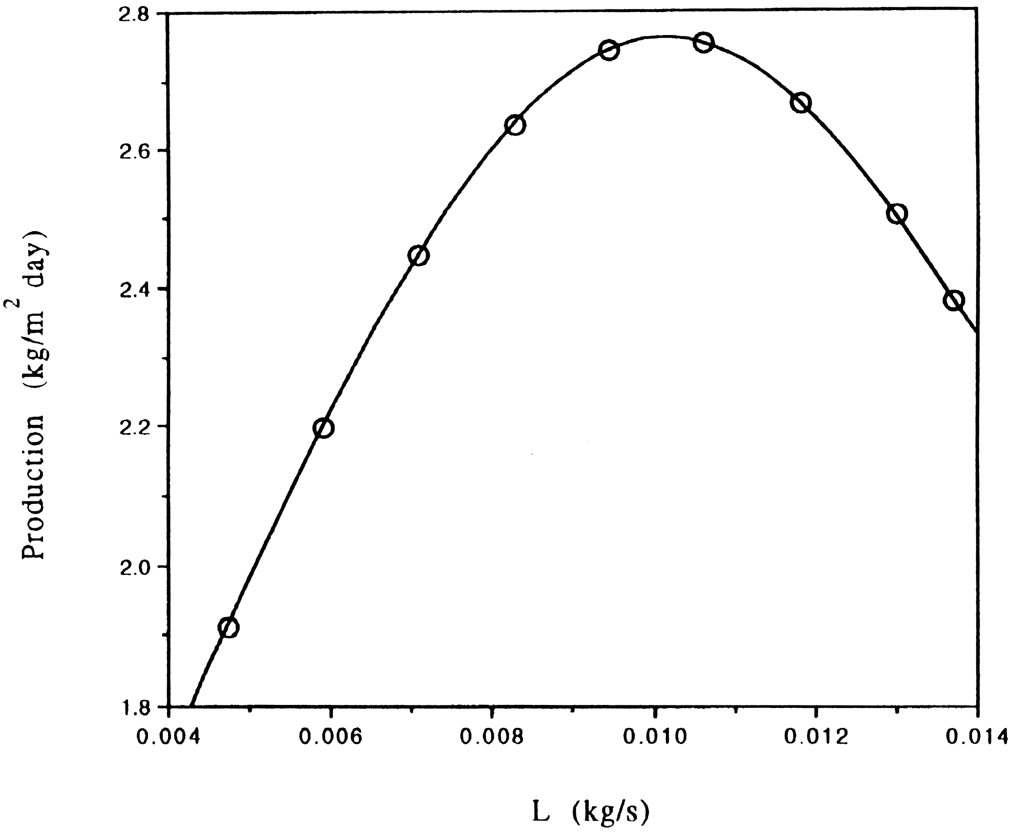

Fig. 15. Simulation study for the effect of water flow rate on the daily production of the unit.

References

[1] Nawayseh NK, Farid MM, Al-Hallaj S, Al-Timimi AR. Solar desalination based on humidification process: I—Evaluating the heat and mass transfer coefficients (in press).

[2] Al-Hallaj S. Solar desalination by humidification–dehumidification cycle. MSc thesis, Jordan University of Science and Technology, Jordan, 1994.

[3] Goff PL, Geoff JL, Jeday MR. Development of a rugged design of a high efficiency multi-stage solar still. Desalination 1991;82:153–63.

[4] Graff JH. Solar desalination plant contra CO_2 emission. Desalination 1991;82:187–96.

[5] Sousa HJ, Janisch V. Solar desalination based on the multi-cycle concept. Desalination 1987;67:75–80.

[6] Chaibi MT, Safi MJ, Hasairi M. Performance analysis of a solar desalination unit in South Tunisia. Desalination 1991;82:197–205.

[7] Khedr M. Techno-economic investigation of an air humidification–dehumidification desalination process. Chem Engng Technol 1993;16:270–4.

[8] Nawayseh NK. Solar water desalination with natural draft air humidification–dehumidification process. MSc Thesis, University Sains Malaysia, Malaysia, 1996.

[9] Stoecker WF, Jones JW. Refrigeration and air conditioning, 2nd ed. New York: McGraw Hill, 1982.

[10] Riggs JB. An introduction to numerical methods for chemical engineers, 2nd ed. Texas Tech University Press, 1994 (Software supplement, Ver. 2.0 IBM).
[11] Hsieh JS. In: Solar energy engineering. New Jersey: Prentice-Hall, 1986. p. 110–47.
[12] Farid MM, Hamad F. Performance of a single-basin solar still. Renewable Energy 1993;3(1):75–83.